

ORIGINAL ARTICLE

Investigation of isothiocyanate release from electrospun modified poly(L-lactic acid)/mustard powder composite fibers

Junyan Yao^{1,2}, Shijie Zhang¹, Loong-Tak Lim³ and Xiao Chen¹

Mustard seed containing glucosinolates can be used as a natural source of antimicrobial volatile isothiocyanate (ITC) through enzymatic hydrolysis. ITC can be used in active food packaging to inhibit the proliferation of spoilage microorganisms. In this study, antibacterial composite fibers were prepared by encapsulating mustard powder (MP) in carrier materials of electrospun poly(L-lactic acid) (PLLA)/poly[(lactic acid)-*co*-lysine] (PLAL) fibers. Uniaxial composite fibers (PLLA/MP, PLLA/PLAL/MP) and coaxial composite fibers (PLLA/PLAL/MP-PLLA, PLLA/MP-PLLA/PLAL) were fabricated by electrospinning, and these fibers could be used to produce a series of volatile antibacterial substances, ITCs, which were extracted by hexane under proper temperature and moisture. The morphologies, chemical structures, thermal properties and hydrophilicities of the electrospun composite fibers were investigated. Ultraviolet spectrophotometry (UV) was used to evaluate the controlled ITC release behaviors from these fibers. The results indicated that the mean particle diameter was 975 ± 126 nm and the main interaction between the MP and the carrier polymers was physical. The addition of MP and PLAL could improve the hydrophilic property of PLLA and change the thermal properties. Different fibers exhibited distinct ITC release behaviors, and the ITC release period of the coaxial fibers (approximately 14 days) was longer than that of the uniaxial fibers (approximately 8 days). These fibers have bright prospects in antibacterial ITC controlled release.

Polymer Journal (2017) 49, 449–456; doi:10.1038/pj.2017.7; published online 22 February 2017

INTRODUCTION

Isothiocyanates (ITCs) are a category of anticancer and antibacterial compounds that can function as bacteriostats to inhibit the growth of bacteria, mold and yeast.^{1–3} This property can be exploited for active packaging applications, especially in inhibiting the growth of microorganisms.^{4,5} However, because of their volatility, ITCs must be encapsulated to prevent premature evaporative loss.^{6,7} Mustards belong to the Cruciferae family and contain large amounts of glucosinolates and β -D-glucosidase (myrosinase), which produce ITCs via an enzyme-catalyzed reaction. Glucosinolates and myrosinase exist independently in plants,^{8,9} and ITCs can be generated when the tissue is damaged. Processed mustard powders (MPs) can thus be used as a natural occurring ITC carrier for antimicrobial food packaging.

Several methods are applied to the analysis of ITC at present, such as high-performance liquid chromatography¹⁰ and gas chromatography.¹¹ These methods can accurately detect individual volatile substances, such as allyl isothiocyanate (AITC), which is one of the ITC. Ultraviolet spectrophotometry (UV) can be used to investigate a series of ITC substances with a mutual functional group, such as AITC, glucocapparin and gluconapin. In this paper, UV was

used to investigate the ITC (the common -N=S=O) release after the MP particles undergo certain pretreatments.

Poly(L-lactic acid) (PLLA) is a biodegradable and biocompatible polymer that can be applied in embedding materials,^{12–16} and PLLA is often blended with other crystalline polymers, such as poly(ethylene oxide) and polycaprolactone, to improve its hydrophilic, thermal and mechanical properties.^{17,18} Because PLLA is a hydrophobic and crystalline polymer, it is necessary to improve its hydrophilicity and increase the size of its amorphous regions for applications in fields, such as drug delivery.¹⁹ Poly[(lactic acid)-*co*-lysine] (PLAL) is an amorphous polymer that possesses improved reactive functionality and hydrophilicity. Blending PLLA/PLAL can significantly improve the hydrophilicity and material properties of PLLA optimized for tissue engineering and drug delivery systems.^{20,21} In particular, the hydrophilicity and amorphous regions of the carrier materials in this experiment are important for moisture absorption and the diffusion of ITC. PLAL is an alkaline polymer that can be used to regulate the pH of a solution by blending with PLLA to a certain range. Electrospun PLLA ultrafine fibers with a large surface area and high porosity have been applied for drug delivery.^{22–24} Coaxial electrospun fibers with a

¹Department of Applied Chemistry, School of Natural and Applied Sciences, Northwestern Polytechnical University, Xi'an, Shaanxi PR China; ²Key Laboratory of Macromolecular Science & Technology of Shaanxi Province, Northwestern Polytechnical University, Xi'an, Shaanxi PR China and ³Department of Food Science, University of Guelph, Guelph, Ontario, Canada

Correspondence: Professor J Yao, Department of Applied Chemistry, School of Natural and Applied Sciences, Northwestern Polytechnical University, Beilin, No. 127 Youyi West Road, Xi'an, Shaanxi Province 710072, PR China.

E-mail: yaojunyan@nwpu.edu.cn

Received 11 November 2016; revised 4 January 2017; accepted 16 January 2017; published online 22 February 2017

Table 1 Parameters and components of electrospun fibers

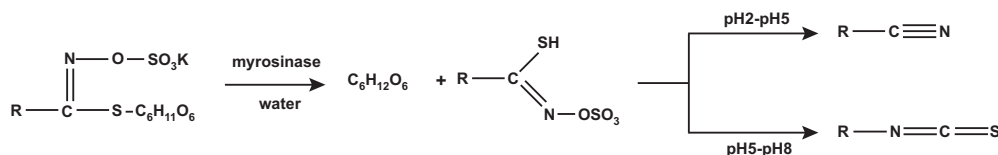
Fibers	PLLA/MP	PLLA/PLAL/MP	(PLLA/MP)–(PLLA/PLAL)	(PLLA/PLAL/MP)–PLLA
MP content in fiber/wt%	50	50	20	20
PLLA content in fiber/wt%	50	35	60	76
PLAL content in fiber/wt%	—	15	20	4
Voltage/kV	16	16	24	22
Collecting distance/cm	18	18	15.5	15.5
Concentration of solutions/wt%	10	10	10 ^a , 10 ^b	10 ^a , 10 ^b
Feed rate/ $\mu\text{l min}^{-1}$	23.60	29.79	8.936 ^a , 17.87 ^b	8.936 ^a , 17.87 ^b

Abbreviations: MP, mustard powder; PLAL, poly(lactic acid)-*co*-lysine; PLLA, poly(L-lactic acid).

^aRepresents core layer.

^bRepresents shell layer.

The first two column fibers represent different uniaxial fibers; third and fourth column fibers are (core)–(shell) coaxial fibers.

**Figure 1** Sketch of the hydrolysis reactions of glucosinolates.

core–shell configuration have been exploited for sustained release applications by controlling the degradation of the shell material.^{25,26}

In the present study, MP was employed as a natural carrier of ITC in various electrospun PLAL/PLLA fiber matrices. Uniaxial (PLLA/MP, PLLA/PLAL/MP) and coaxial composite fibers ((PLLA/PLAL/MP)–PLLA, (PLLA/MP)–(PLLA/PLAL)) were fabricated by electrospinning. The particle size distributions of the MP particles and the morphologies, chemical structures and thermal and hydrophilic properties of these electrospun fibers were analyzed. A simple method for producing and extracting ITC from these composite fibers is introduced in this study, and UV is applied to investigate the controlled release behaviors of the antimicrobial volatile ITC from the fibers.

EXPERIMENTAL PROCEDURES

Materials

PLLA was purchased from Shanghai Leon Chemical, Ltd. (Shanghai, China) with a molecular weight (M_w) of $305 \times 10^3 \text{ g mol}^{-1}$ and a polydispersity index (PDI) of 1.38. PLAL was laboratory-made with an M_w of $19.8 \times 10^3 \text{ g mol}^{-1}$ and PDI of 1.12. AITC was a 94 wt% analytical reagent and was supplied by Alfa Aesar (Shanghai, China). *N,N*-dimethylformamide (DMF) and chloroform were both used as analytical reagents and were provided by the Aladdin Industrial Corporation (Shanghai, China). Hexane, an analytical reagent, was purchased from Guangdong Guanghua Sci-Tech Co., Ltd, Guangdong, China. Mustard seed was purchased from a local supermarket.

Pretreatment of mustard seed

Mustard seeds were ground into fine powders by a vertical planetary ball mill (QM-C1, Nanjing University Instrument Factory, Nanjing, China) with a speed of 480 r min^{-1} for 2 h. The milled MP was then defatted by Soxhlet extraction with hexane at 55°C for 48 h. Next, the defatted MP was sifted (100 mesh) after drying in a vacuum oven at 45°C for 24 h. After two cycles of ball milling (500 r min^{-1} , 2.5 h), defatting and drying (with the same conditions as above), the MP was stored in a desiccator.

Fabrication of electrospun composite fibers

Stock solutions (10 wt%) of PLLA and PLLA/PLAL were prepared by dissolving PLLA and PLLA/PLAL (PLLA:PLAL = 70:30, wt%) in a chloroform/DMF blend (chloroform:DMF = 90:10, wt%). Different amounts of MP particles were

then dispersed in the stock solutions with a magnetic stirrer for 12 h. These suspensions were blended as PLLA50/MP50, PLLA40/MP60 and PLLA28/PLAL12/MP60, with the numbers in the formulas representing the percentages of PLLA, PLAL and MP in blends. These suspensions were treated in an ultrasonic bath for 3 h before being electrospun in an electrospinning machine (SS-2554, UCALERY BEIJING CO., Ltd., Beijing, China). The coaxial spinneret contains two concentric capillaries, while the uniaxial spinneret has only one capillary. In the study, the diameter of the uniaxial spinneret is 0.67 mm, that of the thin capillary in the coaxial spinneret is 0.60 mm and that of the thick capillary is 2.23 mm. These parameters and the components of the fibers are shown in Table 1, as obtained from an optimization process.

Characterization of electrospun composite fibers

A small amount of MP particles was dispersed in hexane, and a laser particle size analyzer (ZEN3600, Malvern Instrument, Ltd., Malvern, UK) was used to determine the particle size distribution of the MP. The morphologies of the electrospun composite fibers were examined using an environmental scanning electron microscope (ESEM) (Quanta200, FEI, Eindhoven, The Netherlands), and their average diameters were measured by Image J (National Institutes of Health, Bethesda, MD, USA).

The chemical character of the composite fibers was evaluated by Fourier transform infrared (FT-IR) spectroscopy (Nicoletis10, Thermo Scientific, Ltd., Waltham, MA, USA) using the thin film method. Stock electrospinning suspensions were coated on the surface of a potassium chloride tablet and then scanned in the $4000\text{--}400 \text{ cm}^{-1}$ wavenumber range after the solvent of the suspensions was thoroughly evaporated.

To analyze the hydrophilicities of the electrospun composite fibers, the contact angle was measured (XG-EV900, Shanghai Semiconductor Technology Co., Ltd., Shanghai, China). The thermal properties of the electrospun fibers were evaluated by differential scanning calorimetry (DSC, METTLER TOLEDO, Ltd., Im Langacher Greifensee, Switzerland). Each sample was cut into a small piece (approximately 3–8 mg). Before testing, the samples were dried at 40°C for 10 h in a vacuum drying oven and then heated at a rate of $10^\circ\text{C min}^{-1}$ from -10 to 250°C in a N_2 atmosphere. The test data were analyzed by TA Universal Analysis 2000 (WATERS TECHNOLOGY SHANGHAI LIMITED, Shanghai, China).

Method design of ITC release

The reaction of the glucosinolates is summarized in Figure 1. MP (0.5 g) was weighed into a clean centrifuge tube, and then 0.5 ml of deionized water was added. At predetermined time intervals, hexane was injected into the centrifuge

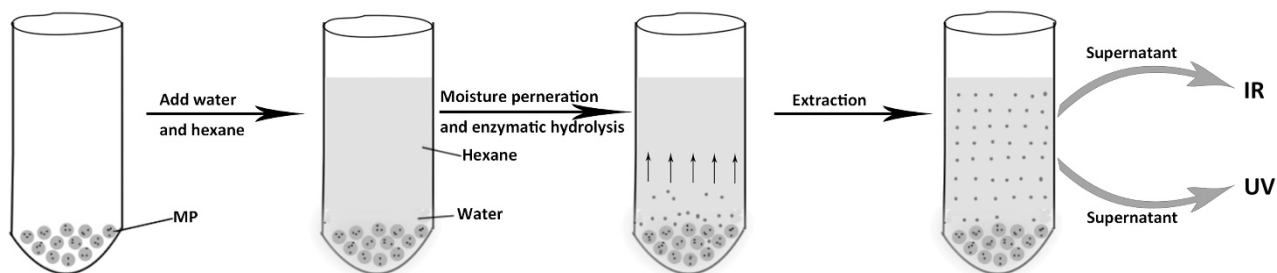


Figure 2 Extraction diagram of ITC with hexane. A full color version of this figure is available at the *Polymer Journal* online.

tube to extract the enzymatic hydrolysate, as shown in Figure 2. After storing for 6 h at 21 °C, the tube was centrifuged at 10 °C for 10 min at 2000 r min⁻¹. The solution had a pH of 6.5 at this time. A series of AITC standard solutions were prepared with hexane as a solvent. The hydrolysis extract solution and AITC standard solutions were analyzed by IR using the liquid membrane method in which 1–2 drops of liquid samples were injected between two pieces of potassium bromide tablets, forming a thin film. The samples and standard solutions were also analyzed using an ultraviolet spectrophotometer (UV-2550, SHIMADZU, Ltd., Kyoto, Japan).

ITC controlled release behavior from electrospun composite fibers

The approach to studying the release of ITC from the electrospun composite fibers was as follows. The fibers were weighed into volumetric flasks, and deionized water (0.5 ml) was added to infiltrate these fibers. Hexane was immediately added to the flask to a total volume of 25 ml. Experiments were carried out at 21 °C, and the pH values of all these hydrolysis solutions were approximately 6.5. The quantitative hydrolysis solution was taken out for UV testing at predetermined time intervals. After each test, an equal amount of hexane was added to the volumetric flask. The cumulative release of ITC could be calculated from Equation 1,

$$\begin{aligned} m_i &= c_i \times v_i \\ m_i' &= c_i \times v_i' + c_{i-1} \times v_{i-1}' + \dots + c_1 \times v_1' \\ M_i &= m_i + m_{i-1}' \end{aligned} \quad (1)$$

where m is the content of ITC in the volumetric flask; c is the concentration of ITC in the volumetric flask; v is the solution volume in the volumetric flask; m' is the content of ITC removed; v' is the removal volume; M is the cumulative release content of ITC; and i represents the i th determination. Each fiber was tested three times and the mean was taken to eradicate any discrepancies.

RESULTS AND DISCUSSION

Size distribution of MP and morphologies of fibers

The size distribution of the MP particles is shown in Figure 3. The average diameter of the MP was 975 ± 126 nm. Approximately 38% of the particles were between 10 and 300 nm in size, and the particles of 300–1000 nm occupied the largest proportion in size, approximately 52%. Approximately 10% of the particles were >1000 nm. The smallest particle was approximately 54 nm, and the largest was approximately 7500 nm.

Figure 4 shows the ESEM micrographs for the electrospun composite fibers. The larger MP particles were in these fibers in the form of beads, and the diameters of these fibers were not uniform. It could be inferred from Figures 3 and 4 that most of the smaller MP particles were embedded in the fibers, and a few were exposed on the surface of the fibers due to the split of the Taylor cone during electrospinning. The MP particles were well dispersed within the carrier materials. The surface of these fibers appeared to be porous under higher magnification. The porous structures give the fibers a greater surface area and stronger adsorptive capacity than nonporous fibers, which could improve the adsorption of moisture on the fiber

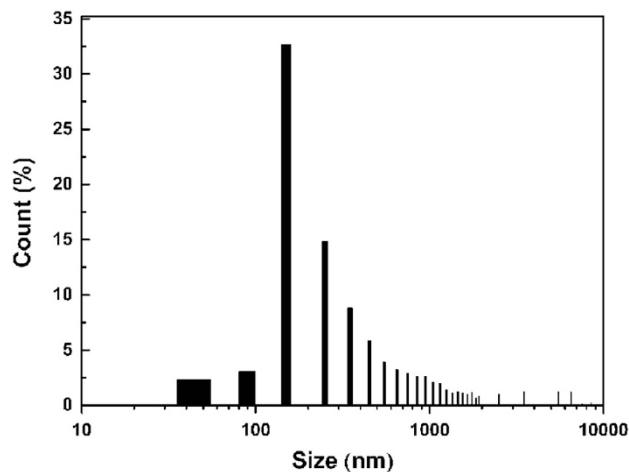


Figure 3 Size distribution of MP particles in the study.

surface and promote the formation and release of ITC. The mean diameters of the uniaxial composite fibers were smaller than those of the coaxial composite fibers due to the smaller diameter of the uniaxial spinning needle compared with that of the coaxial spinning needle. Owing to the addition of the lower M_w PLAL, which could decrease the viscosity of the spinning solution and enhance the electrical conductivity, the uniaxial PLLA/PLAL/MP fiber showed a smaller diameter than the PLLA/MP fiber. The (PLLA/MP)–(PLLA/PLAL) electrospun fibers were finer than the (PLLA/PLAL/MP)–PLLA fibers because of their higher PLAL content due to the faster feed rate of the shell material compared with that of the core material during the electrospinning process.

Chemical character of the electrospun composite fibers

Figure 5 shows the IR spectra of various electrospun fibers. Figure 5A is the IR spectrum of PLLA, showing C=O and C–O stretching bands at 1751 and 1092 cm⁻¹, respectively. The absorption peaks of the PLLA amorphous and crystalline structures were located at 871 and 756 cm⁻¹, respectively. Figure 5F shows the IR spectrum of MP. There were absorption peaks near 3283 and 1539 cm⁻¹ representing the N–H stretching vibration and the amide I band from the protein. The PLAL molecular chain is composed of PLA and polylysine segments containing C=O, –NH₂, –NH–, –OH and other groups. Figure 5B is the IR spectrum of PLLA/MP, which contains an obvious absorption peak at 1539 cm⁻¹ by comparison with Figure 5A. Figures 5C–E represent the IR spectra of these fibers with different structures. The spectral features of Figures 5C–E were similar, and the main characteristic peaks of the individual components did not exhibit significant frequency shift in the spectra of the blends. This implies

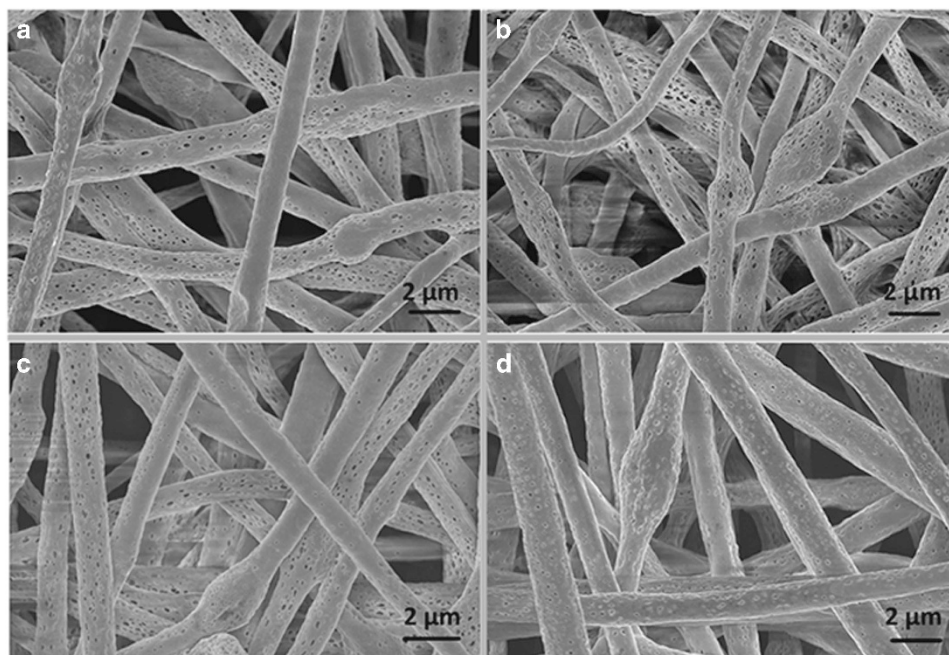


Figure 4 ESEM micrographs of four electrospun MP-loaded fibers. (a) PLLA/MP ($\phi = 947.7 \pm 53$ nm); (b) PLLA/PLAL/MP ($\phi = 917.7 \pm 42$ nm); (c) (PLLA/MP)-(PLLA/PLAL) ($\phi = 1057.7 \pm 83$ nm); (d) (PLLA/PLAL/MP)-PLLA ($\phi = 1089.7 \pm 91$ nm). A full color version of this figure is available at the *Polymer Journal* online.

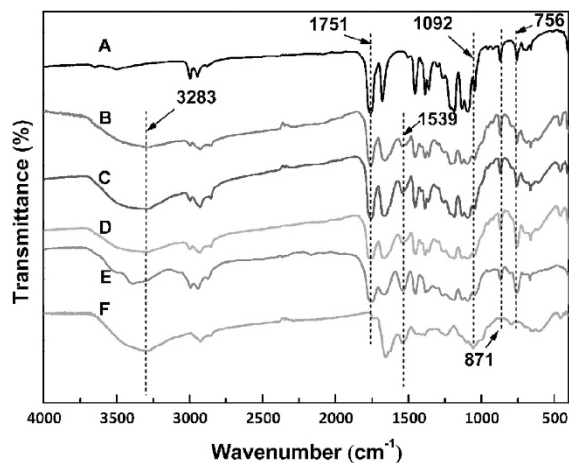


Figure 5 IR spectra of various electrospun fibers. A: PLLA; B: PLLA/MP; C: PLLA/PLAL/MP; D: (PLLA/MP)-(PLLA/PLAL); E: (PLLA/PLAL/MP)-PLLA; F: MP. A full color version of this figure is available at the *Polymer Journal* online.

that there were no new chemical bonds being formed between the MP particles and the carrier materials and that the interactions between these components were mainly physical.

Hydrophilic properties of the electrospun composite fibers

PLLA is a hydrophobic polymer, while PLAL with its hydrophilic amino groups is a hydrophilic/lipophilic polymer. The hydrophilic properties of the electrospun fibers not only affect the biodegradability of the fibers but also influence the enzymatic hydrolysis of the glucosinolates in the MP, thereby affecting the controlled release behavior of the composite fibers. Table 2 shows the results of water contact angle testing.

Table 2 Water contact angles of various fiber membranes

Fiber membrane	Contact angle (°)
PLLA	89.7 ± 1.6
PLLA/MP	65.4 ± 1.4
PLLA/PLAL/MP	43.6 ± 1.3
(PLLA/MP)-(PLLA/PLAL)	54.7 ± 2.1
(PLLA/PLAL/MP)-PLLA	83.6 ± 2.3

Abbreviations: MP, mustard powder; PLAL, poly(lactic acid)-co-lysine; PLLA, poly(L-lactic acid).

The contact angle of the PLLA/MP fiber membrane was lower than that of the PLLA fiber, probably because the MP might contain hydrophilic substances, such as proteins, starch and cellulose. The contact angle of the PLLA/PLAL/MP fiber membrane was the smallest among these fiber membranes, indicating that the hydrophilicity of the fiber membrane could be improved by the addition of PLAL, which will enhance the moisture absorption of the fiber membrane. The shell material of the (PLLA/PLAL/MP)-PLLA coaxial fiber was the hydrophobic PLLA, and the content of PLAL in this fiber was the lowest (approximately 4 wt%), while the content of PLAL in the shell material of the (PLLA/MP)-(PLLA/PLAL) coaxial fiber was approximately 30 wt%. The (PLLA/PLAL/MP)-PLLA coaxial fiber membrane exhibited a larger contact angle than the (PLLA/MP)-(PLLA/PLAL) coaxial fiber membrane, implying that the (PLLA/MP)-(PLLA/PLAL) fiber membrane had a higher surface affinity to moisture. Owing to the split of the liquid jet in electrospinning, small amounts of PLAL and MP could exist on the surface of the (PLLA/PLAL/MP)-PLLA fiber, resulting in the contact angle of the (PLLA/PLAL/MP)-PLLA fiber being less than that of the PLLA fiber. The different hydrophilicities of the fibers result in different moisture absorption abilities, and as moisture is a necessary substance in the enzymatic hydrolysis reaction, their release rates of ITC would be diverse.

Thermal properties of the electrospun composite fibers

The DSC thermograms of the various fibers and their thermal parameters are presented in Figure 6 and Table 3, respectively, showing that the glass transition (T_g) and melting (T_m) temperatures of the PLLA/PLAL fiber (Figure 6B) were lower than those of the PLLA fiber (Figure 6A). This was principally because PLAL is an amorphous polymer with low M_w that has the role of a diluent. The added PLAL likely weakened the intermolecular interactions of the PLLA chains, thereby decreasing the T_g of the PLLA/PLAL fiber. On the other hand, the chain entanglement of the PLAL and PLLA polymers could interfere with the crystallization of PLLA, lowering the T_m of the PLLA fiber.

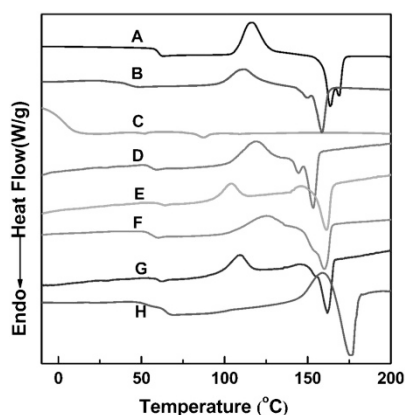


Figure 6 DSC curves of various electrospun fibers. A: PLLA; B: PLLA/PLAL; C: PLAL; D: PLLA/PLAL/MP; E: PLLA/MP; F: (PLLA/MP)–(PLLA/PLAL); G: (PLLA/PLAL/MP)–PLLA; H: MP. A full color version of this figure is available at the *Polymer Journal* online.

Table 3 Thermal parameters of various fibers

Fibers	PLLA	PLLA/PLAL	PLLA/MP	PLLA/PLAL/MP	(PLLA/PLAL/MP)–PLLA	(PLLA/MP)–(PLLA/PLAL)
$T_g/^\circ\text{C}$	57.9	52.8	58.3	54.5	57.2	54.1
$T_m/^\circ\text{C}$	169.8	158.6	161.7	152.3	162.6	160.3

Abbreviations: MP, mustard powder; PLAL, poly[(lactic acid)-*co*-lysine]; PLLA, poly(L-lactic acid).

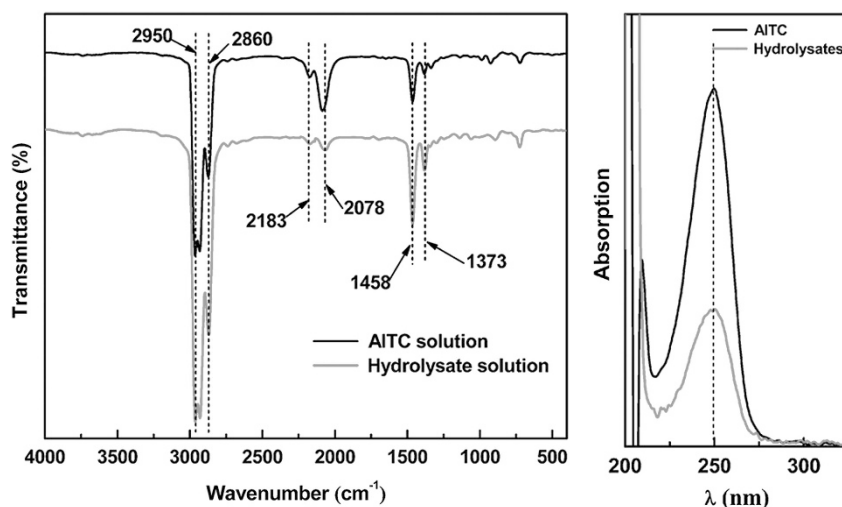


Figure 7 IR and UV spectra of AITC solution and glucosinolate hydrolysates. A full color version of this figure is available at the *Polymer Journal* online.

The MP matrix is complex, and therefore the interpretation of the DSC thermograms of MP is difficult. Proteins and other materials in MP are susceptible to hydrolysis and degradation as the MP is heated to 200 °C. Figure 6D shows the DSC curve of PLLA/PLAL/MP, where it may be observed that the addition of MP particles increased the T_g compared with that of the PLLA/PLAL fiber (Figure 6B). This might be due to the solubilization of some components in the MP particles into the polymer, and the encapsulation effect protects the materials from oxygen/moisture. The T_m of the PLLA/MP fiber (Figure 6E) was lower than that of the PLLA fiber, suggesting that the MP interfered with the chain packing of the PLLA crystalline phases during the electrospinning process. Comparing E, F, G and H in Figure 6, the T_g and T_m of the coaxial fibers changed to smaller degrees than the uniaxial fibers because the PLAL and MP contents in the coaxial fibers were lower. For the same reason, the T_g and T_m of the (PLLA/PLAL/MP)–PLLA coaxial fiber changed by less than that of the (PLLA/MP)–(PLLA/PLAL) coaxial fiber. Furthermore, the contents of MP and PLAL in the PLLA/PLAL/MP fiber were the highest among these composite fibers (referring to Table 1), and the PLLA/PLAL/MP fiber also showed the lowest T_m .

This indicates that the addition of PLAL and MP particles could affect the crystalline phases of the PLLA fibers and thereby influence the ITC diffusion in the matrix and the degradation of the matrix, leading to different release behaviors for the fibers.

ITC controlled release behaviors from the composite fibers

The FT-IR and UV methods were applied to study the enzymatic hydrolysates of the glucosinolates in MP. Typical IR and UV spectra of the AITC solution and enzymatic hydrolysates with hexane as solvent are presented in Figure 7. As shown, the C-H stretching vibration was located at 2980–2800 cm^{-1} and the C-H bending vibration at 1475–1300 cm^{-1} (Figure 7), mainly due to the hexane solvent.

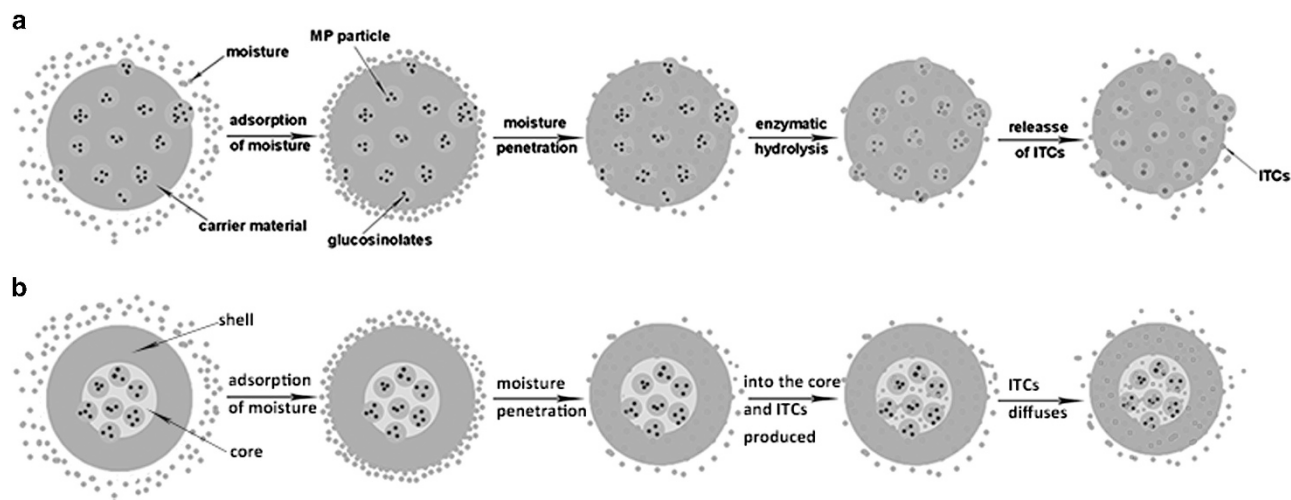


Figure 8 Diagrams of ITC generation from the fibers. (a) uniaxial fiber; (b) coaxial fiber. A full color version of this figure is available at the *Polymer Journal* online.

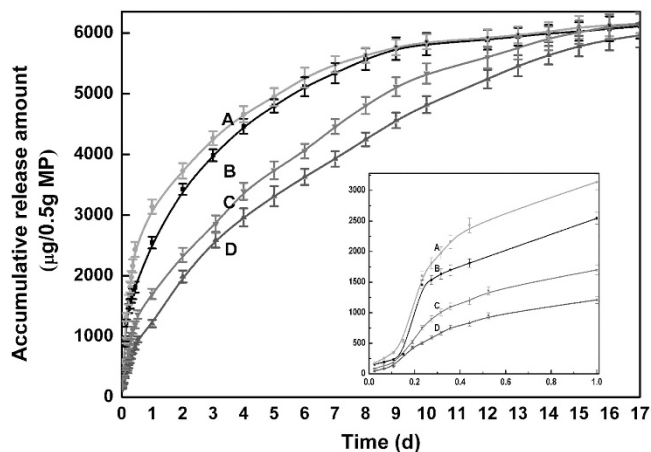


Figure 9 ITC release curves of four electrospun MP-loaded fibers. A: PLLA/MP; B: PLLA/PLAL/MP; C: (PLLA/MP)–(PLLA/PLAL); D: (PLLA/PLAL/MP)–PLLA. A full color version of this figure is available at the *Polymer Journal* online.

The $N=C=S$ vibration bands are the hallmark feature of ITC, located near 2183 and 2078 cm^{-1} , and were observed in the glucosinolate enzymatic hydrolysates with no apparent frequency shift. The spectrum of the glucosinolate enzymatic hydrolysates was in accordance with that of the AITC solution. These observations showed that the hydrolysis products by hexane extraction were mainly ITC. There were no stray peaks in the spectrum of the glucosinolate enzymatic hydrolysates, indicating that only the ITC were present in the enzymatic hydrolysates, without other impurities.

In the UV spectra (Figure 8), the AITC had a clear absorption peak at 248.5 nm , attributable to $N=C=S$ in the *Z*-isomer in the chemical structure of AITC (1-propene, 3-isothiocyanato). Because $N=C$ and $C=S$ are not in the same plane and therefore exhibit a weak π electron conjugation, the absorption peak of AITC was generated by the $n \rightarrow \pi^*$ electronic transition. In contrast with the UV spectrum of AITC, there also appeared an absorption peak at 248.5 nm in the UV spectrum of the glucosinolate enzymatic hydrolysates, and no other miscellaneous peak existed, indicating that the extraction product was the ITC. This result was consistent with that of the IR analysis.

Using 248.5 nm as the characteristic absorbing peak value of the ITC, a standard curve was obtained by linear regression (Equation 2),

$$Abs = 0.01109C - 0.02207 \quad (2)$$

where C was the concentration of ITC and Abs was the absorbance value. By measuring the absorbance value (Abs) of the enzymatic hydrolysates at 248.5 nm using a UV spectrophotometer, the concentration of ITC could be calculated, and the cumulative release amount could be obtained.

The release rate of ITC in uniaxial MP-loaded fibers was mainly dependent on the diffusion through the polymer matrix. On the other hand, the coaxial MP-loaded fiber with a core–shell structure was a reservoir-like storage system with MP particles physically embedded in the core polymer and the shell materials acting as barriers. Therefore, in the latter, the release rate of ITC is mainly dependent on the degradation and erosion of the polymer carriers.^{27,28} The kinetics of the ITC formation are summarized as shown in Figure 8. In the moisture-activated ITC release reaction, water was first adsorbed on the surface of the composite fibers, which depended on the hydrophilicity of the fibers. The moisture penetrates into the fibers by diffusion, which in turn infiltrates the MP particles. This triggered an enzymatic hydrolysis reaction in the glucosinolates, generating ITC. The ITC diffusing toward the surface of the fiber, driven by a concentration gradient, were finally desorbed from the fiber surface to the air. The ITC particularly diffused not only from the uniaxial fibers through the amorphous region of the matrix and the pores produced by the solvent evaporation during electrospinning but were also released from the coaxial fibers through the shell materials. In the subsequent release of both the uniaxial and coaxial fibers, the degradation and erosion of the carrier materials served to complement the channels of ITC release.

Figure 9 shows the ITC release curves of the various electrospun MP-loaded fibers. The ITC release time of MP could be improved by blending with matrix materials with electrospinning. Moisture is needed in the reaction and could affect the formation and release of the ITC. In the initial stage, the moisture needs to penetrate into the MP particles of the fibers, and then the glucosinolate hydrolysis reaction would occur. Thus there was a plateau at the beginning. The ITC started to be generated and released with the immersion in moisture. Owing to the hydrophilic PLAL, the PLLA/PLAL/MP fiber

Table 4 Fitting results of various MP-loaded fibers

Fibers	Fitting results	A_0	B_0	R^2
PLLA/PLAL/MP	$\frac{y}{6130} = 1 - 0.7666e^{-0.2608t} - 0.2545e^{-7.418t}$	0.7666	0.2545	0.9992
PLLA/MP	$\frac{y}{5206} = 1 - 0.6238e^{-0.2318t} - 0.3844e^{-4.357t}$	0.6238	0.3844	0.9995
(PLLA/MP)–(PLLA/PLAL)	$\frac{y}{6876} = 1 - 0.8514e^{-0.1275t} - 0.1419e^{-4.036t}$	0.8514	0.1419	0.9994
(PLLA/PLAL/MP)–PLLA	$\frac{y}{7368} = 1 - 0.8742e^{-0.0922t} - 0.1106e^{-1.736t}$	0.8742	0.1106	0.9995

Abbreviations: MP, mustard powder; PLAL, poly(lactic acid-co-lysine); PLLA, poly(L-lactic acid).

released more ITC than the coaxial fibers with a core-shell structure. Overall, the uniaxial composite fibers exhibited larger cumulative ITC releases than the coaxial fibers within 12 h. The cumulative release amount of the PLLA/PLAL/MP fiber was approximately 2500 µg and that of the PLLA/MP reached 1800 µg. On the other hand, the cumulative release amount of the (PLLA/MP)–(PLLA/PLAL) coaxial fiber reached 1400 µg and that of the (PLLA/PLAL/MP)–PLLA was only 950 µg. For uniaxial fibers, because the glucosinolate hydrolysis occurred near the fiber surface first, the ITC tended to be released quickly from the MP particles. The addition of PLAL increased the hydrophilicity of the PLLA/PLAL/MP fiber, causing a greater release than from the PLLA/MP fiber, which may facilitate the diffusion of moisture into the fiber to activate the hydrolysis of the glucosinolates. Moreover, the matrix material could degrade under conditions of moisture with time, further promoting the formation and release of ITC. The ITC produced from the fibers could diffuse into the amorphous region of the matrix materials. The ITC release rate from the PLLA/PLAL/MP fiber was higher than that of the PLLA/MP fiber. This is because the hydrophilic PLAL could make the composite fiber more easily infiltrated. In addition, the incorporation of the amorphous PLAL could expand the amorphous region of the matrix materials. For the coaxial fibers, some MP particles might be exposed on the external surface of the shell layer because of the fiber splitting during the electrospinning, which led to the release of ITC in the first 12 h. The shell material of the (PLLA/MP)–(PLLA/PLAL) fiber contained a larger proportion of PLAL, making it more hydrophilic than the (PLLA/PLAL/MP)–PLLA fiber. This may explain why the ITC release amount of the (PLLA/MP)–(PLLA/PLAL) coaxial fiber was higher than that of the (PLLA/PLAL/MP)–PLLA coaxial fiber. Moreover, the coaxial fibers released less ITC than the uniaxial fibers, mainly because the core-shell structure of the coaxial fibers provided a stronger moisture barrier than that in their uniaxial counterparts.

Compared with a previous work by Dai and Lim¹¹ performed in a chamber with a fixed moisture level (PLLA/MP, 100% RH), the results were quite similar but slightly different. The duration of the initial plateau became shorter in this study (approximately 2 h) than in the previous work (approximately 5 h) because the fibers can be saturated in deionized water more easily than in a chamber with a fixed moisture level. Furthermore, the release time in this study (approximately 8 days) was longer than that in the previous work (approximately 5 days), and the cumulative releases in this study were greater than those in the previous work, which could be attributed to the glucosinolates in the fibers reacting more effectively in deionized water than in an environment with a fixed moisture level.

A biexponential-biphase kinetics function (Equation 3) can be used to model the drug controlled release behaviors,

$$\frac{Q_t}{M} - 1 = A_0 e^{\alpha t} + B_0 e^{\beta t} \quad (3)$$

where Q_t is the cumulative release of ITC at time t and α and β are the ITC release rate constants. The equation is composed of two parts, representing the fast and slow phases in the release process. B_0/A_0 represents the effect of the slow phase on the fast phase. The fast and slow phases of the function correspond to the diffusion mechanism and the degradation mechanism, respectively.

The regression results are shown in Table 4. The α and β values increase for the fibers upon moving from the top to the bottom of the table, indicating that the initial release rate of ITC in these fibers presented an increasing trend. The absolute values of A_0 were larger than those of B_0 in all the fitting functions, demonstrating that the release of ITC was mainly through a diffusion mode in the early stage and the degradation and dissolution of the fibers had a complementary role in the release of ITC in the late stage.

The release time of the uniaxial fiber was approximately 8 days, while that of the coaxial fiber was approximately 14 days. The ITC in the core-shell fibers can be released slowly by diffusion with the continuous degradation of the shell material. These MP-loaded electrospun fibers should be sprayed with some water before being applied to the headspace antimicrobial packing.

CONCLUSION

In this study, MP particles are encapsulated as precursors of antibacterial ITC within a carrier material or dispersed on the surface of the carrier material, using uniaxial and coaxial composite fibers prepared by electrospinning technology. The interaction of the MP particles and the carrier materials is mainly physical, as indicated by the ESEM and FT-IR analyses. The addition of PLAL and MP particles can increase the hydrophilic properties of the composite fibers. DSC results show that the PLAL and MP particles affect the crystalline phase of the PLLA fibers and thereby influence the ITC controlled release behaviors. UV spectroscopy is introduced to investigate the ITC release from the MP-loaded fibers, and the ITC are extracted by hexane under the proper temperature and moisture. The ITC release rate of the PLLA/PLAL/MP fiber is higher than that of the PLLA/MP fiber because the addition of PLAL can improve the generation and release rate of ITC. The coaxial fibers exhibit lower ITC release rates than the uniaxial fibers due to their core-shell structure. The release time of ITC from the electrospun fiber can be prolonged by using coaxial electrospinning, and thereby the antibacterial time can be increased. The cumulative ITC release of these MP-loaded fibers follows a biexponential-biphase kinetic equation. These composite fibers can be exposed to the package headspaces of fresh fruits and vegetables with proper moisture, and the ITC could be released from these fibers to inhibit the proliferation of spoilage microorganisms.

CONFLICT OF INTEREST

The authors declare no conflict of interest.

- 1 Park, H. W., Choi, K. D. & Shin, I. S. Antimicrobial activity of isothiocyanates (ITCs) extracted from horseradish (*Armoracia rusticana*) root against oral microorganisms. *Biocontrol Sci.* **18**, 163–168 (2013).
- 2 Prawn, A., Saw, C. L. L., Khor, T. O., Keum, Y. S., Yu, S., Hu, L. & Kong, A. N. Anti-NF- κ B and anti-inflammatory activities of synthetic isothiocyanates: effect of chemical structures and cellular signaling. *Chem. Biol. Interact.* **179**, 202–211 (2009).
- 3 Nadarajah, D., Han, J. & Holley, R. Inactivation of *Escherichia coli* O157: H7 in packaged ground beef by allyl isothiocyanate. *Int. J. Food Microbiol.* **99**, 269–279 (2005).
- 4 Suppakul, P., Miltz, J., Sonneveld, K. & Bigger, S. W. Active packaging technologies with an emphasis on antimicrobial packaging and its applications. *J. Food Sci.* **68**, 408–420 (2003).
- 5 Jung, D. C., Lee, S. Y., Yoon, J. H., Hong, K. P., Kang, Y. S., Park, S. R., Park, S. K., Ha, S. D., Kim, G. H. & Bae, D. H. Inhibition of pork and fish oxidation by a novel plastic film coated with horseradish extract. *LWT Food Sci. Technol.* **42**, 856–861 (2009).
- 6 Vega-Lugo, A. C. & Lim, L. T. Controlled release of allyl isothiocyanate using soy protein and poly(lactic acid) electrospun fibers. *Food Res. Int.* **42**, 933–940 (2009).
- 7 Aytac, Z., Dogan, S. Y., Tekinay, T. & Uyar, T. Release and antibacterial activity of allyl isothiocyanate/ β -cyclodextrin complex encapsulated in electrospun nanofibers. *Colloid Surf. B* **120**, 125–131 (2014).
- 8 Fahey, J. W., Zalcmann, A. T. & Talalay, P. The chemical diversity and distribution of glucosinolates and isothiocyanates among plants. *Phytochemistry* **56**, 5–51 (2001).
- 9 Halkier, B. A. & Gershenzon, J. Biology and biochemistry of glucosinolates. *Annu. Rev. Plant Biol.* **57**, 303–333 (2006).
- 10 Tsao, R., Yu, Q., Potter, J. & Chiba, M. Direct and simultaneous analysis of sinigrin and allyl isothiocyanate in mustard samples by high-performance liquid chromatography. *J. Agr. Food Chem.* **50**, 4749–4753 (2002).
- 11 Dai, R. & Lim, L.-T. Release of allyl isothiocyanate from mustard seed meal powder entrapped in electrospun PLA–PEO nonwovens. *Food Res. Int.* **77**, 467–475 (2015).
- 12 Wei, X. F., Bao, R. Y., Cao, Z. Q., Yang, W., Xie, B. H. & Yang, M. B. Stereocomplex crystallite network in asymmetric PLLA/PDLA blends: formation, structure, and confining effect on the crystallization rate of homocrystallites. *Macromolecules* **47**, 1439–1448 (2014).
- 13 Shikunami, Y. & Okuno, M. Bioresorbable devices made of forged composites of hydroxyapatite (HA) particles and poly-L-lactide (PLLA): Part I. Basic characteristics. *Biomaterials* **20**, 859–877 (1999).
- 14 Auras, R. A. in *Poly(Lactic Acid): Synthesis, Structures, Properties, Processing, and Applications (Wiley Series on Polymer Engineering and Technology)* (eds Auras, R. A., Lim, L.-T., Selke, S. E. & Tsuji, H.) (John Wiley & Sons, New Jersey, USA, 2011).
- 15 Tsuji, H. in *Biopolymers. Polyesters III. Applications and Commercial Products* Vol. 4 (eds Doi, Y. & Steinbüchel, A.) 129–177 (Wiley-VCH, Weinheim, Germany, 2002).
- 16 Tsuji, H. Poly(lactide) stereocomplexes: formation, structure, properties, degradation, and applications. *Macromol. Biosci.* **5**, 569–597 (2005).
- 17 Hou, Q., Paul, A. & Shakesheff, K. M. Injectable scaffolds for tissue regeneration. *J. Mater. Chem.* **14**, 1915–1923 (2004).
- 18 Dell'Erba, R., Groeninckx, G., Maglio, G., Malinconico, M. & Migliozi, A. Immiscible polymer blends of semicrystalline biocompatible components: thermal properties and phase morphology analysis of PLLA/PCL blends. *Polymer* **42**, 7831–7840 (2001).
- 19 Anderson, J. M. & Shive, M. S. Biodegradation and biocompatibility of PLA and PLGA microspheres. *Adv. Drug. Deliver. Rev.* **64**, 72–82 (2012).
- 20 Yao, J., Zhang, S., Li, W., Du, Z. & Li, Y. *In vitro* drug controlled-release behavior of an electrospun modified poly (lactic acid)/bacitracin drug delivery system. *RSC Adv.* **6**, 515–521 (2016).
- 21 Yao, J., Zhang, S., Li, W. & Li, Y. Miscibility evaluation of poly(L-lactic acid)/poly (lactic acid-co-lysine) blends. *J. Appl. Biomater. Funct. Mater.* **14**, 230–239 (2016).
- 22 Agarwal, P., Mishra, P. & Srivastava, P. Statistical optimization of the electrospinning process for chitosan/poly(lactide) nanofabrication using response surface methodology. *J. Mater. Sci.* **47**, 4262–4269 (2012).
- 23 Kong, Y., Yuan, J., Wang, Z. & Qiu, J. Study on the preparation and properties of aligned carbon nanotubes/poly(lactide) composite fibers. *Polym. Compos.* **33**, 1613–1619 (2012).
- 24 Nguyen, L. T., Chen, S., Elumalai, N. K., Prabhakaran, M. P., Zong, Y., Vijila, C., Allakhverdiev, S. I. & Ramakrishna, S. Biological, chemical, and electronic applications of nanofibers. *Macromol. Mater. Eng.* **298**, 822–867 (2013).
- 25 Wang, C. *Organic Functional Nanomaterials: High Voltage Electrospinning Technology and Nanofibers* (eds Wang, C. & Lu, X.) (Science Press, Beijing, China, 2011).
- 26 Persano, L., Camposo, A., Tekmen, C. & Pisignano, D. Industrial upscaling of electrospinning and applications of polymer nanofibers: a review. *Macromol. Mater. Eng.* **298**, 504–520 (2013).
- 27 Nie, H., Dong, Z., Arifin, D. Y., Hu, Y. & Wang, C. H. Core/shell microspheres via coaxial electrohydrodynamic atomization for sequential and parallel release of drugs. *J. Biomed. Mater. Res.* **95**, 709–716 (2010).
- 28 Ji, X., Yang, W., Wang, T., Mao, C., Guo, L., Xiao, J. & He, N. Coaxially electrospun core/shell structured poly(L-lactide) acid/chitosan nanofibers for potential drug carrier in tissue engineering. *J. Biomed. Nanotechnol.* **9**, 1672–1678 (2013).